spectra can be interpreted in terms of the ionic structure $(S_2N^+)(SbCl_6^-)$. In the Raman spectrum of the solid the three bands at 333, 293, and 175 cm^{-1} can be readily assigned as ν_1 (A_{1g}), ν_2 (E_g), and ν_3 (T_{2g}) of an octahedral $SbCl_6^-$ ion. As the site symmetry of $SbCl_6^-$ is D_{2h}, the degeneracy of the E_g and T_{2g} modes is lifted and they are observed as a doublet and a triplet, respectively. In the infrared spectrum the band at 320 cm^{-1} may be assigned as ν_3 (T_{1u}) of $SbCl_6^-$. In addition to the above mentioned bands, the most prominent band in the Raman spectrum is that at 688 cm^{-1} which may clearly be assigned as the single Raman-active fundamental of the linear triatomic S_2N^+. The analogous band of the isoelectronic CS_2 molecule is observed at 656.5 cm^{-1}.[21] However, in addition to this band there are two additional bands: a moderately intense band at 766 cm^{-1} and a very weak band at 680 cm^{-1}. The former is assigned as $2\nu_2$ which should normally be very weak but appears to have its intensity enhanced by Fermi resonance with ν_1. A similar band is observed at 648 cm^{-1} in the Raman spectrum of CS_2 and is similarly assigned to $2\nu_2$ enhanced by Fermi resonance with ν_1.[16] The weak band at 680 cm^{-1} can be assigned as ν_1 of the $^{32}S^{34}SN^+$ molecule for which the calculated value of ν_1 is 678 cm^{-1}. The other Raman-inactive but infrared-active fundamentals of the S_2N^+ ion, ν_2 and ν_3, are observed at 374 and 1498 cm^{-1}, respectively, and have frequencies close to the corresponding bands for CS_2. Satisfactory solution Raman spectra of $(S_2N)(SbCl_6)$ could not be obtained due to interference of solvent lines, low solubility, or reaction with the solvent.

Registry No. $(S_2N)(SbCl_6)$, 67556-29-0; S_7NH, 293-42-5; S_7NBCl_2, 67556-30-3; 1,4-$S_6N_2H_2$, 3925-67-5; $SbCl_5$, 7647-18-9.

Supplementary Material Available: A table of the moduli of the observed and calculated structure amplitudes (2 pages). Ordering information is given on any current masthead page.

References and Notes

(1) R. J. Gillespie, D. R. Slim, and J. D. Tyrer, *J. Chem. Soc., Chem. Commun.*, 253 (1977).
(2) H. G. Heal, *J. Chem. Soc.*, 4442 (1962).
(3) M. Becke-Goehring, H. Jenne, and E. Fluck, *Chem. Ber.*, **91**, 1947 (1958).
(4) M. Becke-Goehring, H. Herb, and W. Koch, *Z. Anorg. Allg. Chem.*, **264**, 137 (1951).
(5) H. G. Heal, *Nature (London)*, **199**, 371 (1963).
(6) J. Nelson, *Spectrochim. Acta, Part A*, **27**, 1165 (1971).
(7) All calculations were carried out on a CDC-6400 computer. The programs DATCO3, ABSORB, and DATDRN were used for preliminary treatment of data as was the program NORMSF. The full-matrix least-squares program, CUDLS, and Fourier program, SYMFOU, were written locally by J. S. Stephens and J. S. Rutherford, respectively. The cell diagram was prepared using the program ORTEP by C. K. Johnson, U.S. Atomic Energy Commission Report ORNL 3794, revised June 1965.
(8) Refinements were tried in both space groups *I*222 and *Immm*. Refinement in *I*222 was terminated at $R_1 = 0.0411$, $R_2 = 0.0416$ (630 reflections, 26 variables). All atom parameters were transformed $x, y, z \rightarrow -x, -y, -z$ and refinement in *I*222 was terminated at $R_1 = 0.0414$, $R_2 = 0.0418$. The first refinement proceeded rapidly to a maximum shift/error of 0.02, whereas the second was less rapid and stabilized at a maximum shift/error of 0.16. Nevertheless, the application of the Hamilton test (W. C. Hamilton, *Acta Crystallogr.*, **18**, 502 (1965)) shows that the two refinements are not significantly different. Thus on this basis, and in the absence of any other evidence of an acentric space group (the results from NORMSF can be used as an indicator only and not as direct evidence), we have made the final refinement in the space group *Immm*.
(9) B. Lippert, C. J. L. Lock, B. Rosenberg, and M. Zvagulis, *Inorg. Chem.*, **16**, 1525 (1977).
(10) R. P. Hughes, N. Krishnamachari, C. J. L. Lock, J. Powell, and G. Turner, *Inorg. Chem.*, **16**, 314 (1977).
(11) $R_1 = \sum(|F_o| - |F_c|)/\sum|F_o|$; $R_2 = [\sum w(|F_o| - |F_c|)^2/\sum wF_o^2]^{1/2}$.
(12) A. C. Larson, *Acta Crystallogr.*, **23**, 664 (1967).
(13) (a) D. T. Cromer and J. T. Walker, "International Tables for X-Ray Crystallography", Vol. IV, J. A. Ibers and W. C. Hamilton, Ed., Kynoch Press, Birmingham, England, 1974, Table 2.2A, p 72 ff; (b) D. T. Cromer and J. A. Ibers, ref 13a, Table 2.3.1, pp 149–150.
(14) H. S. Low and R. A. Beaudet, *J. Am. Chem. Soc.*, **98**, 3849 (1976).
(15) R. J. Gillespie, P. R. Ireland, and J. E. Vekris, *Can. J. Chem.*, **53**, 3147 (1975).
(16) A. H. Guenther, T. A. Wiggins, and D. H. Rank, *J. Chem. Phys.*, **28**, 682 (1958).
(17) M. R. Truter, D. W. J. Cruickshank, and G. A. Jeffrey, *Acta Crystallogr.*, **13**, 855 (1960).
(18) E. K. Plyler, L. R. Blaine, and E. D. Tidwell, *J. Res. Natl. Bur. Stand.*, **55**, 183 (1955).
(19) L. Pauling, "Nature of the Chemical Bond," 3rd ed., Cornell University Press, Ithaca, N.Y., 1960.
(20) R. J. Gillespie, "Molecular Geometry", Van Nostrand-Reinhold, London, 1972.
(21) B. Stoicheff, *Can. J. Phys.*, **36**, 218 (1958).

Contribution from the Departments of Chemistry, Baylor University, Waco, Texas 76703, and University of Texas at Austin, Austin, Texas 78712

Crystal Structure and Raman Spectral Study of Ligand Substitution in $Mn_3[Co(CN)_6]_2 \cdot xL$

G. W. BEALL, W. O. MILLIGAN,* J. A. PETRICH, and B. I. SWANSON

Received January 17, 1978

Ligand substitution in the Prussian blue analogue $Mn_3[Co(CN)_6]_2 \cdot xL$ has been studied using X-ray crystallography and Raman spectroscopy. The structure of the methanol-substituted species, $Mn_3[Co(CN)_6]_2 \cdot 12CH_3OH$, is quite similar to the parent hydrated form; the space group is *Fm3m* with $a = 10.550$ (3) Å. The unit cell contains $1^1/_3$ formula units and both coordinated and zeolitic methanol molecules. The coordinated methanol species form $^1/_3$ of the ligand environment of the manganese atoms. The remaining methanols occupy the tetrahedral holes in the lattice and are H bonded to the coordinated methanol species. The final R and R_w values for 137 reflections were 4.4 and 5.2%, respectively. Raman scattering has been employed to study the relative importance of hydrogen-bonding ability and size of L in determining the rate with which various ligands substitute into the lattice. A possible explanation for the semipermeable membrane properties of these compounds has been proposed.

Introduction

The structure of pseudo Prussian blue salts, such as $Mn_3[Co(CN)_6]_2 \cdot xH_2O$, is usually based on a model proposed by Ludi.[1-3] Recently, detailed X-ray and neutron diffraction studies of $Mn_3[Co(CN)_6]_2 \cdot 12H_2O$ have yielded a more satisfactory model of the metal cyanide and the hydrogen-bonded water structure.[4] However, in spite of the several structural studies of the hydrated Prussian blue complexes, there are still questions concerning the zeolitic water structure in these materials. A clear understanding of the water network is essential if we are to properly model the H_2O transport in these semipermeable membranes.

Recently, we reported a single-crystal Raman study of $Mn_3[Co(CN)_6]_2 \cdot xL$ (M = Mn^{II}, Cd^{II}) where H_2O was re-

*To whom correspondence should be addressed at Baylor University.

0020-1669/78/1317-2978$01.00/0

Table I. Positional and Thermal Parameters[a] for $Mn_3[Co(CN)_6]_2 \cdot 12CH_3OH$

atom	x	y	z	B, Å^2	β_{11}	β_{22}	β_{33}	occupancy
Mn	$^1/_2$	$^1/_2$	$^1/_2$	2.98 (5)				1
Co	0	0	0	1.68 (5)				$^2/_3$
C(1)	0	0	0.1780 (8)		55 (2)		49 (4)	$^2/_3$
N	0	0	0.2854 (14)		102 (5)		50 (4)	$^2/_3$
O(1)	0	0	0.2997 (28)		149 (13)		75 (11)	$^1/_3$
C(2)	0.08	0.09	0.230	8.0				$^1/_{24}$
O(2)	0.1829 (27)	0.1829 (27)	0.1829 (27)	9.3 (13)				$^1/_8$
C(3)	0.3129 (93)	0.1871 (93)	0.2440 (156)	6.05 (45)				$^1/_{16}$
O(3)	$^1/_4$	$^1/_4$	$^1/_4$	6.0				$^1/_2$

[a] The temperature factor is of the form $\exp[-(\beta_{11}h^2 + \beta_{22}k^2 + \beta_{33}l^2 + 2\beta_{12}hk + 2\beta_{13}hl + 2\beta_{23}kl)]$, where β_{ij} values are the thermal parameters. β_{12}, β_{13}, and β_{23} are equal to zero.

placed by NH_3.[5,6] The Raman study showed that the metal–cyanide vibrational modes are quite sensitive to the nature of the ligand. In the present study ligand substitutions of $Mn_3[Co(CN)_6]_2 \cdot xL$, where L is H_2O, NH_3, CH_3OH, CH_3CHO, $(CH_3)_2O$, H_2S, PH_3, CH_3SH, and $(CH_3)_2S$, have been studied employing Raman scattering to evaluate relative rates of substitution and the interactions of the various ligands with the transition-metal–cyanide network. In order to further clarify the structure of the ligand network, the structure of the methanol-substituted species has also been solved using X-ray diffraction.

Experimental Section

The crystals were grown by slow diffusion of solutions of $MnCl_2$ and $H_3Co(CN)_6$. A single crystal with the morphology of a regular cube ca. 0.1 mm on edge was then mounted in a 0.2-mm Mark capillary and placed under high vacuum at 70 °C for 24 h to dehydrate it. The dehydrated crystals were then exposed to methanol vapor. The capillary was sealed and mounted on a Syntex $P2_1$ computer-controlled diffractometer equipped with a graphite incident-beam monochromator. Least-squares refinement of 15 centered reflections produced the orientation matrix for room-temperature data collection and gave a cell constant of a = 10.550 (3) Å. Data were collected in the range of $0° < 2\theta < 75°$ using Mo Kα radiation (λ 0.71069 Å). The θ–2θ scan technique with a variable scan from 2.0 to 24°/min was used. Additional details about data collection have been described previously.[7] Three reflections were chosen as standards and monitored every 50 reflections to check stability. A total of 314 reflections with $I > 3\sigma(I)$ were obtained and yielded upon averaging 137 independent reflections. The data were corrected for Lorentz and polarization effects. An absorption correction employing crystal shape was also applied.[8]

The crystals employed in the substitution studies were mounted in a special Raman cell[5] and dehydrated at 65–100 °C under high vacuum for a period of 48 h. The various ligands were admitted to the cell by passing the compounds as gases through a vacuum line from a sample bulb. The pressure of the ligands, determined from a manometer attached to the manifold, was about 100 mmHg. The ligands were removed as described above employing a liquid-nitrogen trap to condense the gas.

The Raman spectra were obtained using a Cary 82 spectrometer and a Spectra Physics Model 164 krypton ion laser (6471-Å line). The laser power was maintained at 100 mW to avoid sample degradation. The slit width was 5 cm^{-1} for the $Co(CN)_6^{3-}$ frequencies and 15 cm^{-1} for the ligand modes.

Structural Refinement

The structural model by Ludi[1] was used as a starting model for the metal, carbon, and nitrogen atoms. After several cycles of refinement, a difference Fourier map yielded possible positions for the methanol molecules. After several additional cycles of refinement, a diffuse maximum at $^1/_4$, $^1/_4$, $^1/_4$ was observed in the difference Fourier map. An oxygen atom was placed at this site at half-occupancy. The structure converged after several cycles to an R of 4.4% and an R_w of 5.2%, where R and R_w are defined as

$$R = \sum||F_o| - |F_c||/\sum|F_o|$$

$$R_w = \sum w^{1/2}||F_o| - |F_c||/\sum w^{1/2}|F_o|$$

where $w = 1/(\sigma(F_o))^2$. The function minimized in the refinements was $\sum w(|F_o| - |F_c|)$.

Table II. Bond Distances (Å) for $Mn_3[Co(CN)_6]_2 \cdot 12CH_3OH$

Mn–N	2.264 (14)	O(1)–C(2)	1.468 (15)
Mn–O(1)	2.113 (29)	O(2)–C(3)	1.52 (10)
Co–C(1)	1.877 (9)	O(1)–O(2)	2.995 (30)
C(1)–N	1.133 (18)		

In the final cycles of refinement the position of the carbon atom of the coordinated methanol was the only parameter that was constrained, because of high correlation with the cyanide carbon. The scattering factors were obtained from Cromer and Mann.[9] Anamolous dispersion corrections, both real and imaginary, were made for all atoms.[10]

Description of the Structure

Crystal packing in the $Mn_3[Co(CN)_6]_2 \cdot 12MeOH$ is dominated by the strong cyanide linkages between the Co and Mn atoms. The Mn atom is the only atom that is not disordered and is in position set 4(b) (0, 0, $^1/_2$). The Co is in position 4(a) (0, 0, 0) and has an occupancy of $^2/_3$. The cyanides are along the cell edges in position set 24(e) (0, 0, x) where x = ca. 0.1780 (8) and 0.2854 (14) for carbon and nitrogen, respectively. The cyanides are disordered analogous to the Co at an occupancy of $^2/_3$. This disorder leaves the Mn with an average coordination of four nitrogens. The coordination sphere of the Mn is filled by the oxygen of the methanol. O(1) is in position set 24(e) (0, 0, x) where x = ca. 0.2997 (28) with an occupancy of $^1/_3$. The carbon end of the methanol is slightly off the cell edge in position set 96(k) (x, y, z) pointing toward the tetrahedral hole. There is an additional methanol hydrogen bonded to the coordinated methanol. The O(2) of this methanol is along the threefold axis of the cell in position set 32(f) (x, x, x) where x = ca. 0.1829 (27) and has an occupancy of $^1/_8$ (4 atoms). The carbon corresponding to this oxygen is in a general position 192(l) (x, y, z). These positions substantiate the structure proposed by Beall et al. for the hydrated species. Both of the above methanol molecules occupy the vacant Co site. When the structure is completely ordered, which occurs approximately $^1/_3$ of the time, there is an additional methanol molecule at $^1/_4$, $^1/_4$, $^1/_4$ similar to the zeolytic water that is found in $Mn_3[Co(CN)_6]_2 \cdot 12H_2O$. In the water structure it was a simple matter to place the oxygen in the 8(c) position at $^1/_3$ occupancy. For the methanol-substituted species there were no discrete individual peaks for oxygen and carbon but instead only a diffuse peak for their average positions. To approximate the methanol contained in this hole a single oxygen O(3) was placed in the 8(c) position at $^1/_2$ occupancy to compensate for both the carbon and oxygen. Table I lists the positional and thermal parameters for all atoms in the structure.

The bond distances are all quite reasonable (Table II). The Co–C distance of 1.89 (1) Å is similar to that found in $Cs_2LiCo(CN)_6$.[11] The C–N distance of 1.17 (2) Å is within experimental error of that found in the $Cs_2LiCo(CN)_6$ salt. Some interesting changes occur in the Mn–N distance. The change in lattice constant from 10.435 (3) for the water structure to 10.550 (3) for the methanol structure can be

Table III. Raman Frequencies (cm^{-1}) for $Mn_3[Co(CN)_6]_2 \cdot xL$

	L												
mode[a]	*b*	*c*	H_2O	...	MeOH	Me_2O	H_2S	MeSH	Me_2S	D_2S	NH_3	PH_3	MeCHO
ν_1 (A_{1g}, CN)	2151	2162	2190.3	2201.4	2187.5	2195.4	2193.0	2195.2	2190.7	2194.0	2187.6	2193.0	2190.3
ν_3 (E_g, CN)	2137	2151	2171.4	2178.0	2168.5	2174.5	2172.6	2174.2	2171.9	2175.6	2170.9	2174.5	2170.0
ν_{10} (F_{2g}, CoCN)	482	485	?	487							~485		
ν_2 (A_{1g}, CoC)	410	431	485	502.5	474.5	490.5	486.0	494.5	479.5	490.0	475.8	482.0	480.5
ν_4 (E_g, CoC)	?	418	445								464		
ν_{11} (F_{2g}, (CoC)	115	190	196.8	218.5	208.2	208.5	202.7	207.5	198.6	200.6	198.3	198.5	210.0
				180.5									

[a] Reference 12. [b] Frequencies for $Co(CN)_6^{3-}$ taken from ref 13. [c] Frequencies for $Cs_2LiCO(CN)_6$ taken from ref 14.

attributed to the Mn–N distance change and the size of the methanol molecule. This change is most likely a combination of the difference in σ-donor properties and size of methanol molecule that affects the Mn–N bond. The methanol structure appears to be less strained than the water structure. It is likely that the larger methanol molecule fills the vacant holes better. It has been observed that the water-substituted crystals give strain patterns under polarized light, whereas the methanol crystals are isotropic. One possible explanation here is that in the hydrated crystals the distance between manganese atoms in the disordered portion of the structure is smaller than that in the ordered portion of the structure. In the methanol-substituted case these two distances are essentially the same and the crystal strain patterns disappear.

Ligand substitution in $Mn_3[Co(CN)_6]\cdot xL$ has also been probed using Raman scattering. The ligands selected in the Raman study cover a wide range of hydrogen-bonding ability and size. Table III contains a list of all of the ligands employed and the corresponding Raman modes of the metal–cyanide framework. The ligand modes are extremely weak and in most instances were not observed, by virtue of the extremely small size of the crystal used in the Raman study. The vibrational assignments for the metal–cyanide framework have already been discussed.[6]

The metal–cyanide modes are strongly influenced by the ligand. As water is removed, the stretching modes increase in frequency and the F_{2g} symmetry C–Co–C deformation, ν_{11}, splits into two well-resolved bands. The increase in frequency of the stretching modes has been attributed to increased Mn–N interaction resulting from removal of the coordinated water.[5,6] As other ligands are introduced into the lattice, the Raman modes of the metal–cyanide framework return to approximately the same position as that observed for the hydrated sample (Table III). There appears to be a correlation of the σ-donor strength of the ligand and the frequency position observed for the stretching modes. Ligands with poor σ-donor strength exhibit frequencies intermediate to those observed from the hydrated and dehydrated samples (for example, Me_2O and MeSH, Table III). Those ligands with better σ-donor strength than water exhibit stretching modes with frequencies lower than those of the hydrated sample (MeOH and NH_3 in Table III). The suggestion of enhanced L–Mn σ interactions in the case of the methanol-substituted species is consistent with the larger lattice constant and Mn–N distance observed for this salt (above). Also the C–O stretch is observed to decrease in going from the ligand phase (1035 cm^{-1})[12] to the $Mn_3[Co(CN)_6]_2 \cdot 12MeOH$ lattice (996 cm^{-1}) as is consistent with the formation of an O–Mn interaction.

The sensitivity of the C–N stretching modes to the presence of coordinated ligands suggested that the rates of diffusion of L into the $Mn_3[Co(CN)_6]_2$ lattice could be monitored by following the frequencies of these modes as a function of exposure to the ligand. Given the experimental difficulties of observing the Raman spectra as a function of time, such studies can only be expected to give a crude measure of the relative diffusion rates of the ligands. The C–N stretch region

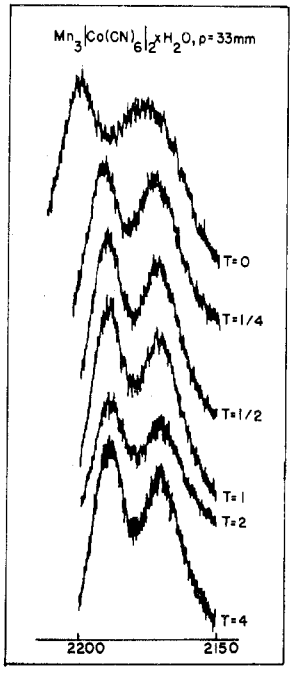

Figure 1. Raman spectra vs. time (h) of exposure to H_2O, ν_1 and ν_3.

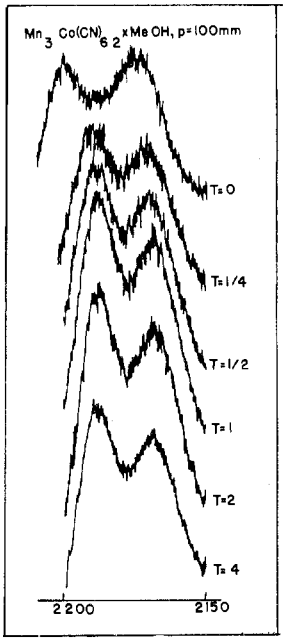

Figure 2. Raman spectra vs. time (h) of exposure to MeOH, ν_1 and ν_3.

is sketched as a function of time of exposure to H_2O, MeOH, and H_2S in Figures 1–3. For both the hydrated and MeOH-substituted samples the C–N stretching modes had

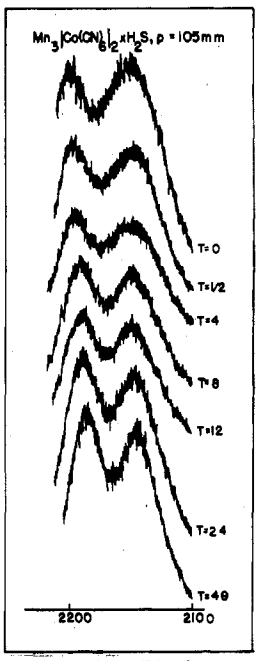

Figure 3. Raman spectra vs. time (h) of exposure to H_2S, ν_1 and ν_3.

shifted to their final positions within 0.5 h after exposure of the anhydrous sample to the ligands. The relatively rapid uptake of H_2O and MeOH should be contrasted with the slow diffusion observed for H_2S (Figure 3). Similar experiments for the remaining ligand resulted in a qualitative ordering as follows: $H_2O \simeq NH_3 \simeq CH_3OH > MeCHO > Me_2O > H_2S \simeq PH_3 \simeq MeSH > Me_2S$. The implication here is that ligands with good hydrogen-bonding capabilities enter the lattice faster. It is interesting to note that large ligands such as MeOH diffuse into the lattice more rapidly than smaller ligands with poor hydrogen-bonding abilities (H_2S, PH_3).

From the above qualitative rates it is clear that hydrogen-bonding ability is more important than size in determining the rate of transport into the vacant lattice. However, the size of the channels (ca. 7 Å) establishes an upper limit on the size of an entering ligand. On the basis of the structure of the hydrated sample, where hydrogen bonding occurs in the region of the coordinated H_2O, it may be inferred that σ-donor properties of the ligand are also important in determining the transport rate in these materials. Unfortunately, it is not possible to separate the effects of σ-donor and hydrogen-bonding abilities since those ligands which hydrogen bond well are also good σ donors; despite this difficulty, we propose the following model for transport into the dehydrated $Mn[Co(CN)_6]_2$ lattice. The initial entering ligands bind to the coordinatively unsaturated Mn atoms. Additional ligands then attach to the coordinated ligands through the formation of hydrogen bonds. Through successive breaking and reforming of the hydrogen bonds these new ligands migrate to coordinatively unsaturated Mn atoms further from the surface of the crystals. Once the network of hydrogen-bonded and coordinated ligands is established, transport may be affected through hydrogen bonding above.

Acknowledgment. We acknowledge the Robert A. Welch Foundation for its support of this research (Grant AA-668 (G.W.B. and W.O.M.) and F-620 (B.I.S. and J.A.P.)).

Registry No. $Mn_3[Co(CN)_6]_2 \cdot 12CH_3OH$, 67464-33-9; $Mn_3[Co(CN)_6]_2 \cdot xH_2O$, 29259-42-5; $Mn_3[Co(CN)_6]_2 \cdot xNH_3$, 57450-35-8; $Mn_3[Co(CN)_6]_2 \cdot xCH_3CHO$, 67464-34-0; $Mn_3[Co(CN)_6]_2 \cdot (CH_3)_2O$, 67464-18-0; $Mn_3[Co(CN)_6]_2 \cdot xH_2S$, 67464-19-1; $Mn_3[Co(CN)_6]_2 \cdot xPH_3$, 67464-20-4; $Mn_3[Co(CN)_6]_2 \cdot xCH_3SH$, 67464-21-5; $Mn_3[Co(CN)_6]_2 \cdot x(CH_3)_2S$, 67464-22-6; $Mn_3[Co(CN)_6]_2 \cdot xCH_3OH$, 67464-23-7; $Mn_3[Co(CN)_6]_2 \cdot xD_2S$, 67478-85-7.

Supplementary Material Available: A listing of observed and calculated structure factors (1 page). Ordering information is given on any current masthead page.

References and Notes

(1) A. Ludi, H. U. Güdel, and M. Ruegg, *Inorg. Chem.*, **9**, 2224 (1970).
(2) V. G. Ron, A. Ludi, and P. Engel, *Chimia*, **27**, 77 (1973).
(3) A. Ludi and H. V. Güdel, *Helv. Chim. Acta*, **51**, 2006 (1968).
(4) G. W. Beall, W. O. Milligan, J. Korp, and I. Bernal, *Inorg. Chem.*, **16**, 2715 (1977).
(5) B. I. Swanson, *Inorg. Chem.*, **15**, 253 (1976).
(6) J. J. Rafalko, B. I. Swanson, and L. H. Jones, *J. Chem. Phys.*, **67**, 1 (1977).
(7) F. A. Cotton, B. A. Frenz, G. Dogonelto, and A. Shaver, *J. Organomet. Chem.*, **50**, 227 (1973).
(8) The absorption program used is a modification of the original by W. R. Busing and H. A. Levy.
(9) D. T. Cromer and H. Mann, *Acta Crystallogr., Sect. A*, **24**, 321 (1968).
(10) D. T. Cromer, *Acta Crystallogr.*, **18**, 17 (1965).
(11) B. I. Swanson and R. R. Ryan, *Inorg. Chem.*, **12**, 283 (1973).
(12) B. I. Swanson, paper presented at the International Raman Conference, Bowden, Me., August 1974.
(13) L. H. Jones, M. N. Memering, and B. I. Swanson, *J. Chem. Phys.*, **54**, 3761 (1970).
(14) B. I. Swanson and L. H. Jones, *J. Chem. Phys.*, **53**, 3761 (1970).